Computer Assisted Mechanics and Engineering Sciences, **13**: 513–521, 2006.
Copyright © 2006 by Institute of Fundamental Technological Research, Polish Academy of Sciences

Adaptive analysis of inelastic problems with Bodner–Partom constitutive model

Witold Cecot
Cracow University of Technology, ul. Warszawska 24, 31-155 Kraków, Poland

(Received in the final form October 6, 2006)

The Bodner–Partom elastic-visco-plastic constitutive equations [4] were used for numerical analysis of inelastic problems. This rate-dependent model makes it possible to describe elastic, plastic and viscous processes in metals, including temperature and continuum damage effects. The adaptive finite element method [9] was applied to approximate solution of the governing equations with two a posteriori error estimates that control accuracy of time and space discretization of displacements and internal variables. The paper addresses a further development of the methodology proposed by the author in previous works [7, 8] and used in [6]. We present here certain additional theoretical background and propose a novel strategy of adaptation as well as verify the method of solution transfer.

Keywords: h-adaptive finite element method, error estimate, elastic-visco-plasticity

1. Introduction

The rate-dependent Bodner–Partom equations have been already integrated using the adaptive finite element method by Bass and Oden [3], Min, Tworzydło and Xiques [18], as well as by the author and Rachowicz [7, 8]. In this paper we present further development and verification of the error estimate, adaptation strategy and the solution transfer after the mesh refinement.

The processes modeled in this monograph are considered as: isothermal, quasi-static, with small displacements and their gradients, and with neglected body forces. The Bodner–Partom [4] constitutive equations belong to the family of unified models i.e. they are based on the supposition that rate-dependent and rate-independent parts of inelastic strains are non-separable. The inelastic strain rate is determined in this model by the following equations

$$\dot{\varepsilon}^*_{ij} = D_o \frac{s_{ij}}{\sqrt{J_2}} \exp\left\{ -\frac{1}{2} \left[\frac{\sqrt{3J_2}}{Z} \right]^{-2n} \right\}, \tag{1}$$

$$\dot{Z} = m_1 (Z_1 - Z) \dot{W}^*, \qquad \dot{W}^* = \sigma_{ij} \dot{\varepsilon}^*_{ij}, \tag{2}$$

where: s_{ij} represent components of deviatoric part of the stress tensor, $J_2 = \frac{1}{2} s_{mn} s_{mn}$, Z stands for the internal variable, responsible for isotropic hardening, with initial value denoted by Z_0. Equation (1) refers to the simplest version of the model and makes use of seven material constants: $E, \nu, Z_0, Z_1, D_o, n, m_1$.

The following semi-weak formulation defines the problem we consider

Find field of displacement rate $\dot{\boldsymbol{u}}(\boldsymbol{x}, t) \in V$ such that for every time instant $\tau \in [0, T]$

$$\int_\Omega C_{ijkl}\, \varepsilon_{ij}(\boldsymbol{v})\, \dot{\varepsilon}_{kl}(\dot{\boldsymbol{u}})\, \mathrm{d}\Omega = \int_{\partial\Omega_N} \hat{\dot{t}}_i\, v_i\, \mathrm{d}s + \int_\Omega 2\mu\, \dot{\varepsilon}^*_{ij}\, \varepsilon_{ij}(\boldsymbol{v})\, \mathrm{d}\Omega \qquad \forall \boldsymbol{v} \in V_o, \tag{3}$$

where $V = \{\boldsymbol{v} \in (H^1)^n;\ \boldsymbol{v} = \hat{\dot{\boldsymbol{u}}}$ on $\partial\Omega_D\}$, $V_o = \{\boldsymbol{v} \in (H^1)^n;\ \boldsymbol{v} = 0$ on $\partial\Omega_D\}$, $\dot{\varepsilon}^*_{ij} \in L^2(\Omega)$ is given by Eq. (1), the initial conditions for $\boldsymbol{u}$, $\boldsymbol{\varepsilon}^*$, Z are compatible with the boundary values

$\hat{t}_i$ on $\partial\Omega_N$ and $\hat{\boldsymbol{u}}$ on $\partial\Omega_D$ that in turn are understood in the sense of traces of H^1 functions, $\mathbf{C}$ is the tensor of elastic material constants, μ is the Lame constant.

2. Approximation of the solution by the adaptive FEM

Mesh adaptivity becomes especially important when large time dependent nonlinear problems are analyzed. The selective mesh refinement should be based on a reliable error estimates since discretization error can be unpredictable by heuristic means.

The numerical solutions of the problems discussed in this paper were obtained by computer programs that make use of the adaptive finite element method proposed in [9, 19, 21]. In particular the kernel of *2Dhp* code [10] has been employed. Its basic routines (data structure, mesh generation, integration of element stiffness matrices, frontal solver, mesh refinement) have been supplemented with the appropriate modules defining the problems, driving the solution algorithms, performing a posteriori error estimates and refinement strategy. Thus, we use

- triangle elements with second order hierarchical shape functions ($p = 2$ at every element),
- h-adaptive mesh refinement based on subdivision (partitioning) of selected elements into smaller ones by h-4 technique shown in Fig. 1a.
- 1-irregular nodes (Fig. 1b) with constraint approximation [9] that provides continuous FEM solution, therefore uniqueness and convergence of the numerical results are assured.

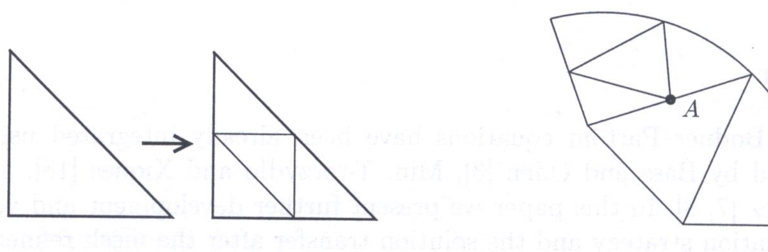

Fig. 1. h-4 refinement and an example of 1-irregular mesh with the constraint (hanging, irregular) vertex node A

The following key components of the adaptive approach are discussed in this Section: error estimate (in time and space), strategy of the mesh adaptation and transfer of the solution to the new mesh.

2.1. Time step control

Integration in time is carried out by the semi–implicit (known also as improved or trapezoid) Euler method with automatic time–step control proposed by Kumar and co-workers [13].

Certain numerical tests have revealed that, for the problem considered, this simple scheme is more efficient than the sophisticated Bulirsh–Stoer or higher order Runge–Kutta approaches [8].

2.2. Error estimate in space accounting for inelasticity

As usual, the approximation error $\boldsymbol{e} \in V$ is defined as

$$\boldsymbol{e} = \boldsymbol{u} - \boldsymbol{u}^X \tag{4}$$

where: $\boldsymbol{u}, \boldsymbol{u}^X$ are the exact and approximate solutions, respectively.

We use the explicit residual estimate [2] in order to bound a norm of the error norm. In the standard version it leads to the error indicator attributed to each finite element ω_k in the form

$$\eta_k^r = \sqrt{h_k^2 \|\mathbf{R}\|^2_{L_2(\omega_k)} + \frac{1}{2} h_k \|\mathbf{J}\|^2_{L_2(\partial\omega_k)}} \tag{5}$$

where $\boldsymbol{R}$ denotes residuum of the governing equation in the considered element, $\mathbf{J}^* = \mathbf{J}$ in $\overline{\Omega} \setminus \partial\Omega_N$ and $\mathbf{J}^* = 2\mathbf{J}$ on $\partial\Omega_N$, $\boldsymbol{J}$ represents the flux jump along the element boundary.

The error estimate mentioned above accounts for only space discretization of displacements. In the case of inelastic problems plastic or visco-plastic deformations are the additional quantities (despite of displacements) that are approximated in the numerical analysis. Thus, the quality of this approximation should be considered in the error analysis. Methods concerning this issue are discussed in many papers.

Most frequently the smoothed gradients of inelastic strains are employed [11] by an analogy with smoothing of stresses in elasticity. In another heuristic approach Sandhu and Liebowitz [23] use ratio of the maximum and average values of either the effective stress or effective plastic strain as an error indicator. Ladeveze [15] suggests verification of the Drucker postulate on statically and kinematically admissible numerical solutions. The method has been generalized for materials with softening [14]. In another approach Stein and Schmidt [25] propose to control the yield condition at certain points that do not coincide with the Gauss integration nodes. Also the dual solution may be used to asses the error for the elastic-plastic problems as it is proposed in [22]. Johnson and Hansbo [12] extended the explicit residual approach for inelastic problems by weighting the resulting error indicator with the L_1-norm of increment of the total strain.

None of the above enumerated methods seemed to be fully adequate for our purposes. The smoothing technique may give false results [20], the Drucker postulate does not always hold, the Bodner–Partom model does not make use of the yield function and the additional dual solution is time consuming. Thus, we propose another approach (presented initially in [7, 8]) and motivated as follows.

The inelastic strains contribute to the right-hand side of our problem. Their accuracy at the Gauss integration points is controlled by the variable time step. However, unless this "loading" is properly represented in space domain (not only at the Gauss points), the solution may be far from the exact one.

In the residual estimate we are able to evaluate only an approximation of the residual due to the interpolation of the right hand side. Therefore, an additional term in the residual estimator shall be introduced.

Formally, we have by simple algebra and the triangle inequality

$$\|\boldsymbol{R}(\boldsymbol{u}^X_{|K})\| = \|\boldsymbol{L}(\boldsymbol{u}^X_{|K}) + \boldsymbol{f}_{|K}\| = \|\boldsymbol{L}(\boldsymbol{u}^X_{|K}) + \boldsymbol{f}^X_{|K} - \boldsymbol{f}^X_{|K} + \boldsymbol{f}_{|K}\| \leqslant \|\boldsymbol{R}^X(\boldsymbol{u}^X_{|K})\| + \|\boldsymbol{f}_{|K} - \boldsymbol{f}^X_{|K}\| \tag{6}$$

where $\boldsymbol{R}^X = \boldsymbol{L}(\boldsymbol{u}^X_{|K}) + \boldsymbol{f}^X_{|K}$ represents the approximation of the residual in which interpolant $\boldsymbol{f}^X$ of the right hand side is used instead of the exact right hand side that in turn has the form

$$f_i = 2\mu\varepsilon^*{}_{ij,j}\,. \tag{7}$$

Usually, the interpolation of inelastic parameters is constructed by using the Gauss quadrature points [24] since, at these points accuracy of fluxes is better than at the element nodes[1]. We assumed the second order elements with 3 Gauss points. Thus, the plastic parameters are approximated by the piecewise linear polynomials and consequently the right hand side $\boldsymbol{f}$ is approximated by the piecewise constant functions.

Consequently, the residual error estimate shall be evaluated as

$$(\eta_k^r)^2 = h_k^2 \|\mathbf{R}^{\mathbf{X}}\|^2_{L_2(\omega_k)} + h_k^2 \|\boldsymbol{f}_{|K} - \boldsymbol{f}^X_{|K}\|^2_{L_2(\omega_k)} + \frac{1}{2} h_k \|\mathbf{J}^*\|^2_{L_2(\partial\omega_k)}\,. \tag{8}$$

[1]It is reported in [26] the most accurate points for second order triangles are the middles of the edges but this observation has been done for particular examples with regular meshes and other shape functions then used by us.

The problem of using a projection of the right hand side instead of its exact value is considered in another contexts (a priori estimation of the residual) in [1, 5].

We propose here to estimate the new term in the explicit residual estimate by the bounding theorem of the interpolation theory which states that whenever the interpolated function has bounded derivatives of order $p+1$, the following inequality holds,

$$\|\boldsymbol{f}_{|K} - \boldsymbol{f}^X_{|K}\|^2_{L_2(\omega_k)} \leq C h^{p+1} |\boldsymbol{f}|_{p+1,\omega_k}\,, \tag{9}$$

where p denotes the order of interpolation and C stands for an unknown constant. Therefore, in the case of inelastic problems we use the following extended residual error indicator,

$$(\eta^r_k)^2 = h^2_k \|\mathbf{R}^{\mathbf{X}}\|^2_{L_2(\omega_k)} + h^3_k |\boldsymbol{f}|^2_{1,\omega_k} + \frac{1}{2} h_k \|\mathbf{J}^*\|^2_{L_2(\partial\omega_k)}\,, \tag{10}$$

where by making use of Eq. (7),

$$|\boldsymbol{f}|^2_{1,\omega_k} = 2\mu \sum_{i,j} \int_{\omega_k} \sum_{|\boldsymbol{\lambda}|=2} \left(\frac{\partial^{|\boldsymbol{\lambda}|} \varepsilon^*_{ij}}{\partial x_1^{\lambda_1} \partial x_2^{\lambda_2}} \right)^2 . \tag{11}$$

The second derivatives of inelastic strains are evaluated by the moving least square technique [16, 17].

2.3. Strategy of mesh adaptation

Various strategies of mesh adaptation may be used. We have chosen fixed fraction approach, i.e. refinement or unrefinement of specified fractions of elements. Such a strategy prevents creation of a large number of new elements during a single refinement.

Since a posteriori error estimates make use of the actual solution the error indicators are evaluated with precision dependent on the solution accuracy. Therefore, the adaptation process is a non-linear task. Consequently, optimal (or close to optimal) mesh may be obtained only in an iterative way.

After a mesh refinement or unrefinement the time integration is performed at the new Gauss points and accuracy of the space approximation changes. We use the adaptation strategy for integration of the rate-dependent models that assumes a re-analysis of small parts of the load history. Whenever the mesh is refined the second run over certain time intervals (δt) helps to avoid the situation when the error done in one time interval influences the accuracy of the further solution. On the other hand the adaptive time stepping prevents from the excessive error cumulation in time integration. δt may be assumed in a wide range. We usually assume it as one tenth of the time interval between the previous and present mesh adaptations.

2.4. Mapping of the solution

The solution mapping may be easily performed when the mesh is refined by subdivision of elements. Only the internal variables and inelastic strains are mapped from the old mesh to the new one. The former quantities are used to evaluate all necessary rates while the inelastic strains uniquely define actual displacements, strains and stresses.

All fields to be transfered are approximated by the Lagrange polynomials (L^m) with the interpolation nodes assumed at the Gauss integration points. After h-4 refinement (Figs. 2) the solution values at the new nodes are easily computed since, all the new interpolation points belong to one old element. Thus, we have a straightforward mapping

$$\phi^{\text{new}}_{ij}(x,y) = \sum_{m=1}^{3} L^m(x,y)\, \phi^{\text{old}}_{ij}(\boldsymbol{b}_m) \tag{12}$$

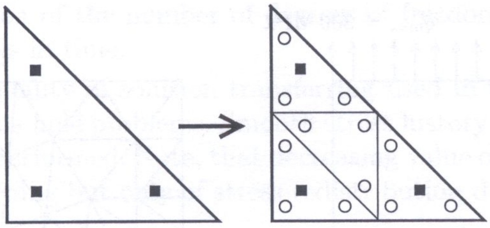

Fig. 2. h-4 refinements; old and new interpolation points for inelastic parameters

that does not alter the transferred function. However, it is worth mentioning that even though the field of internal parameters remains unchanged during such a mapping the resulting, numerically evaluated displacements may not coincide with the solution on the old mesh due to altering of discretization. In order to avoid significant influence of the mesh adaptation on the numerical analysis a re-analysis of small parts of the load history (over the already mentioned time interval δt) is carried out whenever the mesh is adapted.

On the other hand, unrefinement is done wherever these parameters have small second derivatives (are distributed almost linearly). Consequently, unrefinement introduces controlled disturbances in the load history. The difference between the transfered and original fields may be easily computed and if it is too large the unrefinement may be canceled.

3. Numerical tests

The following tests have been performed to verify the proposed error estimates: thick walled cylinder subject to internal pressure, sheet with a hole, and railroad rail.

The following material constants (for a steel) were assumed during the analysis: $E = 207\,\text{GPa}$, $\nu = 0.3$, $Z_0 = 1435\,\text{MPa}$, $Z_1 = 1900\,\text{MPa}$, $D_o = 10^8$, $n = 1.73$, $m_1 = 0.06\,\text{MPa}^{-1}$.

For the cylinder problem, considered as the plane strain state (Fig. 3), the adaptive mesh refinement significantly reduces the number of necessary unknowns (even 2–3 times) as it was already reported in [7] for a similar inelastic problem.

For the sheet with a hole (Fig. 4) an example of adaptively refined mesh and convergence of solution are demonstrated in Fig. 5. Since the number of dof varied during the computations the average number of unknowns is shown in the plot of convergence. The solution obtained on a fine mesh (about 40 000 dof) was used as the reference one.

The convergence tests confirm effectiveness of the adaptive approach. Smaller reduction of the number of dof than in the cylinder problem [7] is observed because the reference uniformly refined mesh is also adapted, in a sense (Fig. 4), due to the domain shape and mesh generation technique.

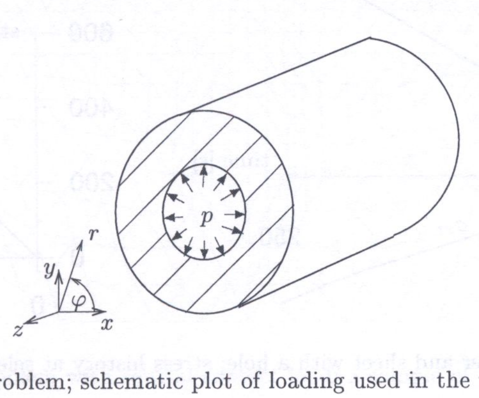

Fig. 3. Cylinder test problem; schematic plot of loading used in the tests (p – internal pressure)

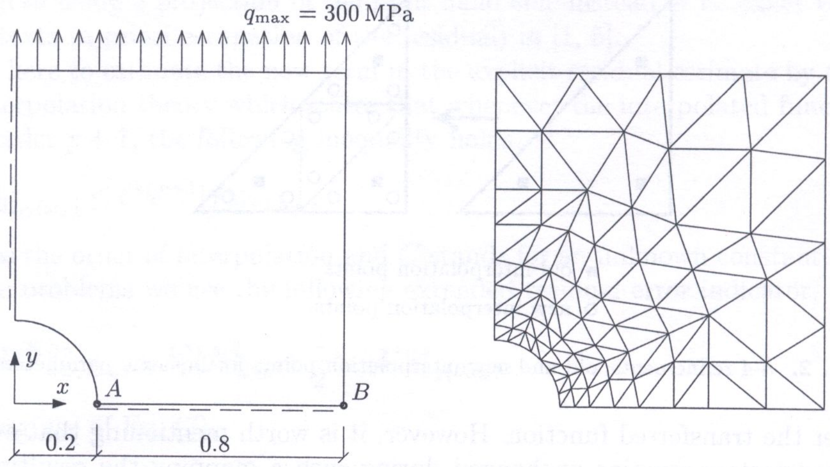

Fig. 4. Sheet with a hole; data for one quarter (dimensions in [m]) of the domain and initial FEM mesh (128 elements, 289 nodes) – plane stress state

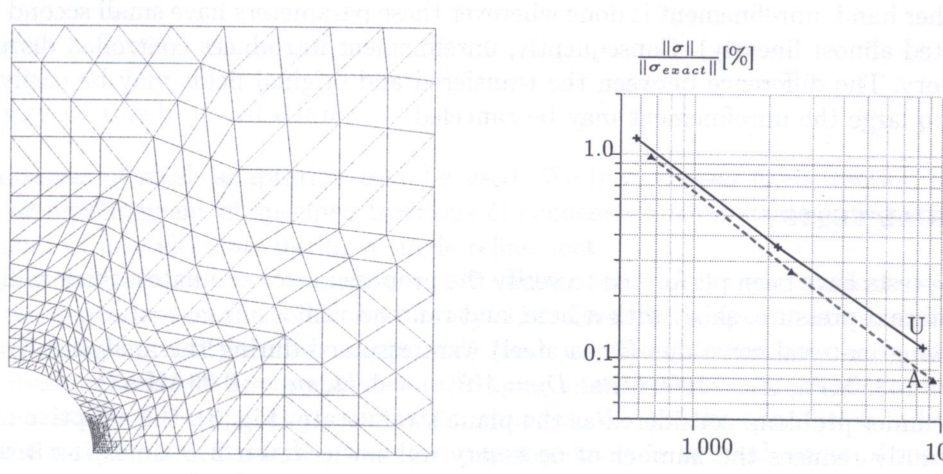

Fig. 5. Sheet with a hole; adaptively refined mesh and convergence tests for second order elements: energy norm of the solution error (logarithmic scale) versus number of scalar degrees of freedom (N), for uniform (U) and adaptive (A) mesh refinements

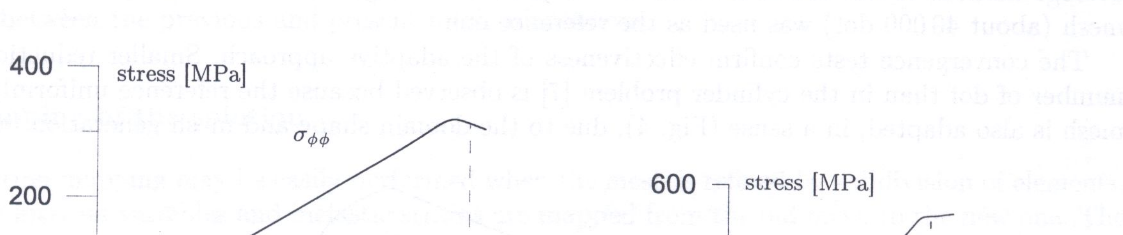

Fig. 6. Cylinder and sheet with a hole; stress history at selected points

However, even a small reduction of the number of degrees of freedom results, for the step-by-step analysis, in a significant savings in time.

In Fig. 6 we demonstrate quality of solution transferring used in the adaptive process for both the cylinder and the sheet with a hole problems. Smooth stress history is observed at time instant T_a when the refinement has been performed. Note, that decreasing value of one of the stress components is not a result of material softening but only of stress redistribution during the increase of the yield zone.

Next, an infinitely long railroad rail is considered. It is loaded here by somewhat unusual loading, i.e. by infinitely long one (Fig. 7). Additionally, the rail is fixed at the bottom in such a way that, 2D plane strain modeling may be assumed. A few adaptive mesh refinements resulted in discretizations, with about 60000 dof, shown in Fig. 8. It enabled approximating the solution with error less than 3% (error estimated by comparison of solutions obtained on two different meshes). One may observe that the automatically refined mesh has the largest density along the border between the plastic and elastic zones. The convergence tests confirm that such refinement, based on an appropriate error estimation, significantly improves convergence [7].

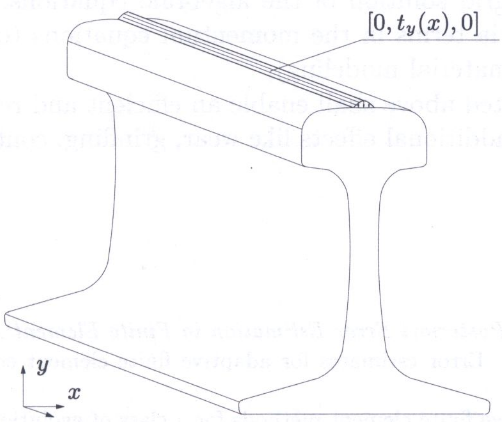

Fig. 7. Rail test problem; a portion of infinitely long rail, $t_y^{\max} = -1\,\text{MPa}$

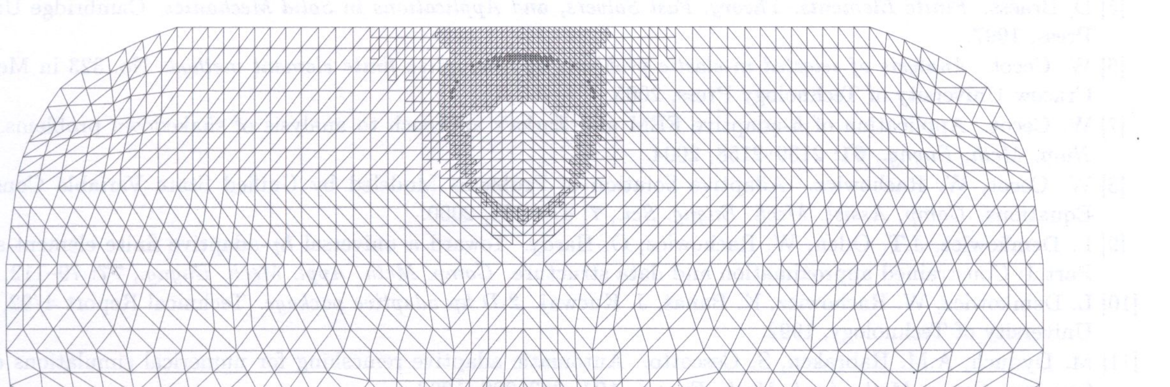

Fig. 8. Railroad rail problem with central contact load; a sample of an adaptively refined mesh

4. Concluding remarks

Efficient integration of the Bodner–Partom model requires adaptive approach. We control accuracy of the approximation by specially generalized explicit residual error estimator. In fact, each error estimate should be generalized in a similar manner, whenever it is used for inelastic problems. The proposed strategy of mesh adaptation and mapping of solution to a new mesh have proved to work properly, especially when re-computation over a certain time interval is used after each mesh adaptation. The area where the mesh has to be refined is automatically detected by the appropriate error estimation.

The mesh refinement by subdivision of elements, rather then by the remeshing technique makes the solution transfer much easier. Therefore, even though the subdivision of elements results in a complex constraint approximation we recommend this type of the adaptive procedure.

The numerical experiments in which we studied efficiency of different schemes of integration in time confirmed that the first order implicit methods are suitable for the Bodner–Partom model. However, a more efficient scheme of integration in time would be welcome.

The further open questions and challenges in the topics of this paper include: making use of *hp* adaptivity, parallel, multigrid solution of the algebraic equations, assessment of the modeling error done by neglecting inertia terms in the momentum equations (quasi-static versus dynamical loading with rate-dependent material modeling),

Completion of the tasks listed above shall enable an efficient and reliable approximation of rate-dependent 3D solutions with additional effects like wear, grinding, continuum damage, temperature influences accounted for.

References

[1] M. Ainsworth, J.T. Oden. *A Posteriori Error Estimation in Finite Element Analysis.* J. Wiley & Sons, 2000.

[2] I. Babuška, W.C. Rheinboldt. Error estimates for adaptive finite element computations. *Int. J. Num. Meth. Engng.*, **12**: 1597–1615, 1978.

[3] J.M. Bass, J.T. Oden. Adaptive finite element methods for a class of evolution problems in viscoplasticity. *Int. J. Engng. Sci.*, 25(623-653), 1987.

[4] S.R. Bodner, Y. Partom. Constitutive equations elastic viscoplastic strain-hardening materials. *J. Appl. Mech.*, **42**: 385–389, 1975.

[5] D. Braess. *Finite Elements. Theory, Fast Solvers, and Applications in Solid Mechanics.* Cambridge University Press, 1997.

[6] W. Cecot. *Analysis of selected in-elastic problems by h-adaptive finite element method.* No. 323 in Mechanics. Cracow University of Technology Press, 2005.

[7] W. Cecot. Application of *h*-adaptive FEM and Zarka's approach to analysis of shakedown problems. *Int. J. Num. Meth. Engng.*, **61**: 2139–2158, 2004.

[8] W. Cecot, W. Rachowicz. Adaptive Solution of Problems Modeled by Unified State Variable Constitutive Equations. *Comp. Assist. Mech. Engng. Sci.*, **7**: 479–492, 2000.

[9] L. Demkowicz, J.T. Oden, W. Rachowicz, O. Hardy. Toward a universal *hp*-adaptive finite element strategy. Part 1: Constrained approximation and data structure. *Comp. Meth. Appl. Mech. Engng.*, **77**: 79–112, 1989.

[10] L. Demkowicz, W. Rachowicz, K. Banaś, J. Kucwaj. *2-D hp adaptive package.* Technical Report 4/92, Cracow University of Technology, 1992.

[11] M. Dyduch, A.M. Habraken, S. Cescotto. Automatic adaptive remeshing for numerical simulations of metal forming. *Comp. Meth. Appl. Mech. Engng.*, **101**: 283–298, 1992.

[12] C. Johnson, P. Hansbo. Adaptive finite element methods in computational mechanics. *Comp. Meth. Appl. Mech. Engng.*, **101**: 143–181, 1992.

[13] V. Kumar, M. Morjaria, S. Mukherjee. Numerical integration of some stiff constitutive models of inelastic deformation. *ASME J. Engng. Mater Technol.*, **102**: 92–96, 1980.

[14] P. Ladeveze, N. Moes, B. Douchin. Constitutive relation error estimators for (visco)plastic analysis with softening. *Comp. Meth. Appl. Mech. Engng.*, **176**: 247–264, 1999.

[15] P. Ladeveze, J.P. Pelle, P. Rougeot. Error estimate procedure in the finite element method and application. *SIAM J. Numer. Anal.*, **20**: 485–509, 1983.

[16] P. Lancaster, K. Salkauskas. Surface generated by moving least squares methods. *Mathematics of Computation*, **155**(37): 141–158, 1981.

[17] T. Liszka, J. Orkisz. The finite difference method at arbitrary irregular grids and its applications in applied mechanics. *Comp. Struct.*, **11**: 83–95, 1980.

[18] J.B. Min, W.W. Tworzydło, K.E. Xiques. Adaptive finite element methods for continuum damage modeling. *Comp. Struct.*, **58**: 887–900, 1995.

[19] J.T. Oden, L. Demkowicz, W. Rachowicz, T.A. Westermann. Toward a universal *hp*-adaptive finite element strategy. Part 2: A posteriori error estimation. *Comp. Meth. Appl. Mech. Engng.*, **77**: 113–180, 1989.

[20] S. Prudhomme, J.T. Oden. Computable error estimators and adaptive techniques for fluid flow problems. In: *Error Estimation and Adaptive Discretization Methods in Computational Fluid Dynamics*, pp. 207–268. Springer, 2001.

[21] W. Rachowicz, J.T. Oden, L. Demkowicz. Toward a universal *hp*-adaptive finite element strategy. Part 3: Design of *hp* meshes. *Comp. Meth. Appl. Mech. Engng.*, **77**: 181–212, 1989.

[22] S. Repin, L. Xanthis. A posteriori error estimation for elasto-plastic problems based on duality theory. *Comp. Meth. Appl. Mech. Engng.*, **138**: 317–339, 1996.

[23] J.S. Sandhu, H. Liebowitz. Examples of adaptive FEA in plasticity. *Engng. Fract. Mech.*, **50**: 947–956, 1995.

[24] J.C. Simo, T.J.R. Hughes. *Computational Inelasticity.* Springer-Verlag, 1998.

[25] E. Stein, ed. *Error-Controlled Adaptive Finite Elements in Solid Mechanics.* J. Wiley & Sons, 2003.

[26] O.C. Zienkiewicz, J.Z. Zhu. Superconvergence and the superconvergent patch recovery. *Finite Elements in Analysis and Design*, **19**: 11–23, 1995.